ISSN 0036-0236, Russian Journal of Inorganic Chemistry, 2017, Vol. 62, No. 5, pp. 591–597. © Pleiades Publishing, Ltd., 2017.
Original Russian Text © Z.T. Gasanova, L.F. Mashadieva, Yu.A. Yusibov, M.B. Babanly, 2017, published in Zhurnal Neorganicheskoi Khimii, 2017, Vol. 62, No. 5, pp. 592–598.

Phase Equilibria in the Cu_2S–Cu_3AsS_4–S System

Z. T. Gasanova[a], L. F. Mashadieva[b], Yu. A. Yusibov[c], and M. B. Babanly[b, *]

[a] *Baku State University, ul. akademika Zakhida Khalilova 23, Baku, AZ 1148 Azerbaijan*
[b] *Institute of Catalysis and Inorganic Chemistry, National Academy of Sciences of Azerbaijan, pr. Dzhavida Guseina 29, Baku, AZ 1143 Azerbaijan*
[c] *Ganja State University, pr. Geidara Alieva 159, Baku, AZ 2000 Azerbaijan*
**e-mail: Babanly_mb@rambler.ru*

Received June 22, 2016

Abstract—Phase equilibria in the Cu_2S–Cu_3AsS_4–S system were studied by differential thermal analysis and X-ray powder diffraction. Important plots characterizing this system were constructed, namely, the *T–x* diagrams of the lateral quasi-binary systems Cu_2S–Cu_3AsS_4 and Cu_3AsS_4–S, some internal sections, the isothermal section of the phase diagram at 300 K, and the projection of the liquidus surface. The fields of primary crystallization of phases and the types and coordinates of in- and monovariant equilibria were found. A wide region of separation of liquid phases was detected in the system.

DOI: 10.1134/S0036023617050126

The Cu–As–S system is of great interest because ternary compounds and glassy alloys in this system are valuable functional materials with semiconductor, photoelectric, optical, and other practically important properties [1–3]. Moreover, almost all of the known ternary compounds in this system occur in nature as minerals and are of considerable interest for Earth geochemistry [4, 5].

Numerous literature data on phase equilibria in the Cu–As–S and the properties of ternary phases in this system were generalized in a review paper [3]. However, their analysis shows that, although a number of polythermal sections have been studied, the full picture of phase equilibria in the system have not yet been determined. A schematic projection of the liquidus surface constructed by Rikel et al. [3] using the published data [6–9] has serious disadvantages: because of the insufficiency of experimental data, the fields of primary crystallization of most phases were delineated conditionally, no isotherms were presented on them, and neither were the accurate coordinates of invariant equilibrium points, etc. The schematicity and contradictoriness of this diagram were also noted by Müller and Blachnik [10, 11].

In the context of the above, we undertook a new detailed investigation of phase equilibria in the Cu–As–S system. Previously [12, 13], we studied phase equilibria in the Cu–Cu_2S–As subsystem and the thermodynamic properties of copper arsenic sulfides. In this work, we explore phase equilibria in the Cu_2S–Cu_3AsS_4–S subsystem.

The phase diagrams of the boundary binary system Cu–S that were presented in modern handbooks [14, 15] virtually coincide. According to available data, in the system, the compounds Cu_2S, Cu_9S_5, and CuS form. The first of them melts congruently at 1403 K; the second exists below a temperature of 345 K, at which it decomposes by a solid-phase reaction; and the third melts with decomposition by a peritectic reaction at 780 K. The compound Cu_2S undergoes polymorphic transformations at 376 and 708 K: the low-temperature modification has the orthorhombic structure, the intermediate modification has the hexagonal structure, and the high-temperature modification has the cubic structure. This compound has the homogeneity region toward an excess of sulfur, which is maximal at ~800 K and is 33.3–36.6 at. % S [14].

In the Cu_2S–S subsystem, the liquidus consists of a single curve describing the primary crystallization of the high-temperature modification of Cu_2S. The liquidus curves of CuS and elemental selenium and also the corresponding invariant equilibria are degenerate. In the system, there is a wide region of separation of two liquid phases, which at the monotectic equilibrium temperature 1086 K extends from 40.1 to 99.8 at. % S [13, 14].

The compound Cu_3AsS_4 melts congruently at 970 K and crystallizes in the orthorhombic (mineral enargite) or tetragonal (luzonite) structure [2, 3].

The crystallographic parameters of copper sulfides and Cu_3AsS_4 according to various authors are available in the literature [2–4, 14–16].

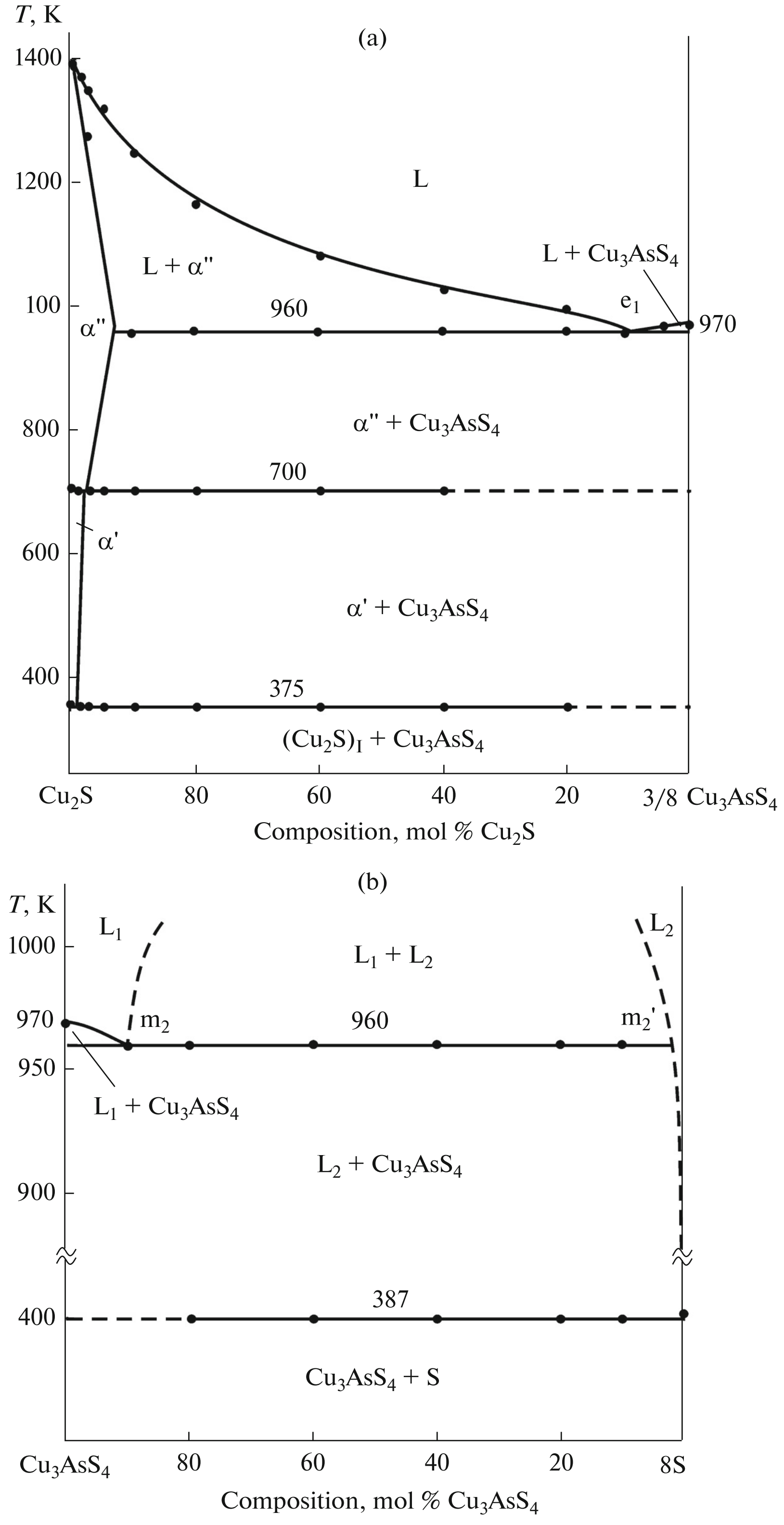

Fig. 1. Quasi-binary systems (a) Cu_2S–Cu_3AsS_4 and (b) Cu_3AsS_4–S.

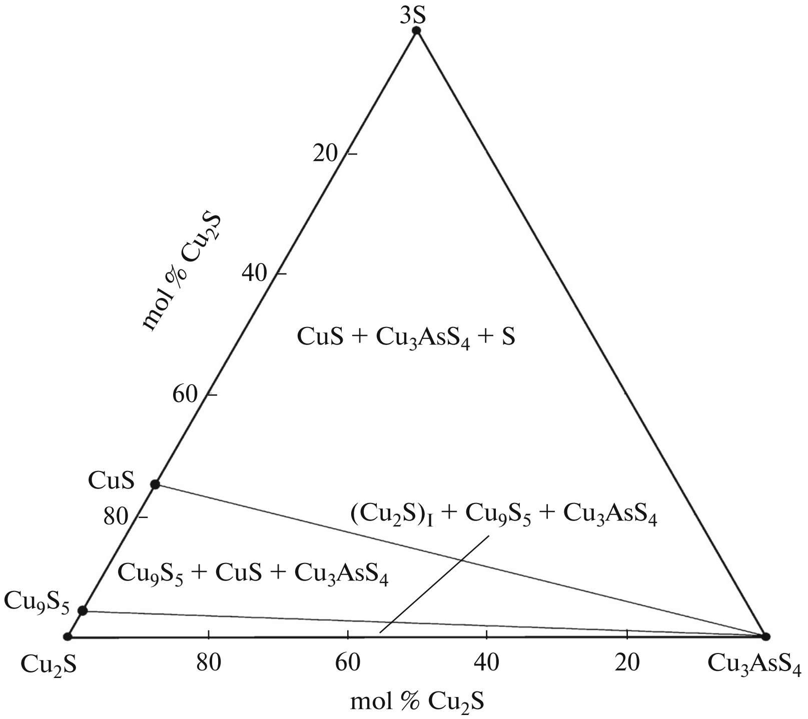

Fig. 2. Diagram of solid-phase equilibria in the Cu_2S–Cu_3AsS_4–S system at 300 K.

EXPERIMENTAL

The compounds Cu_2S, CuS and Cu_3AsS_4 were synthesized by alloying high-purity elemental components in necessary ratios in sealed evacuated (~10^{-2} Pa) quartz ampules. Cu_2S and Cu_3AsS_4 were produced in a two-zone inclined furnace. The temperature of the lower, "hot", zone was 1420 K (Cu_2S) or 1000 K (Cu_3AsS_4), and the temperature of the upper, "cold", zone was 650 K, which is somewhat below the sulfur boiling point (718 K [17]). To obtain homogeneous Cu_2S of the stoichiometric composition, according to a published recommendation [18], the synthesis was followed by quenching from 1300 K into cold water.

Because CuS melts incongruently, the ampule after alloying the components at ~900 K was slowly cooled to a temperature of 700 K, at which annealing was performed for 500 h.

The individuality of the synthesized compounds was checked by differential thermal analysis and X-ray powder diffraction analysis.

Alloys in the Cu_2S–Cu_3AsS_4–S system were produced by alloying the preliminarily synthesized compounds and elemental sulfur in evacuated quartz ampules. By differential thermal analysis of nonhomogenized cast alloys of selected compositions, the temperatures of annealing (at ~30–50 deg below the solidus) were determined, at which the alloys were treated for 600–800 h.

The differential thermal analysis was performed with a NETZSCH 404 F1 Pegasus system, and X-ray powder diffraction analysis was carried out with a Bruker D8 ADVANCE diffractometer.

RESULTS AND DISCUSSION

Processing of the set of the obtained experimental data using published data on the binary system Cu_2S–S gave a mutually consistent picture of phase equilibria in the Cu_2S–Cu_3AsS_4–S subsystem. For the convenience of comparison with the total *T–x–y* diagram of the Cu–As–S system, the composition in the studied subsystem was represented as $Cu_2S\text{–}\frac{3}{8}Cu_3AsS_4\text{–}3S$.

Lateral Quasi-Binary Systems

$Cu_2S\text{–}\frac{3}{8}Cu_3AsS_4$ System (Fig. 1a) has the phase diagram of the eutectic type. The eutectic has the composition 10 mol % Cu_2S and crystallizes at 970 K. The solubility based on the high-temperature modification of Cu_2S (α'') at the eutectic temperature is maximal and is ~6 mol %, and the solubility based on the intermediate modification (α') is ~3 mol %. The formation of solid solutions based on Cu_2S is accompanied by a decrease in the temperatures of polymorphic transitions to 700 and 375 K, at which the eutectoid

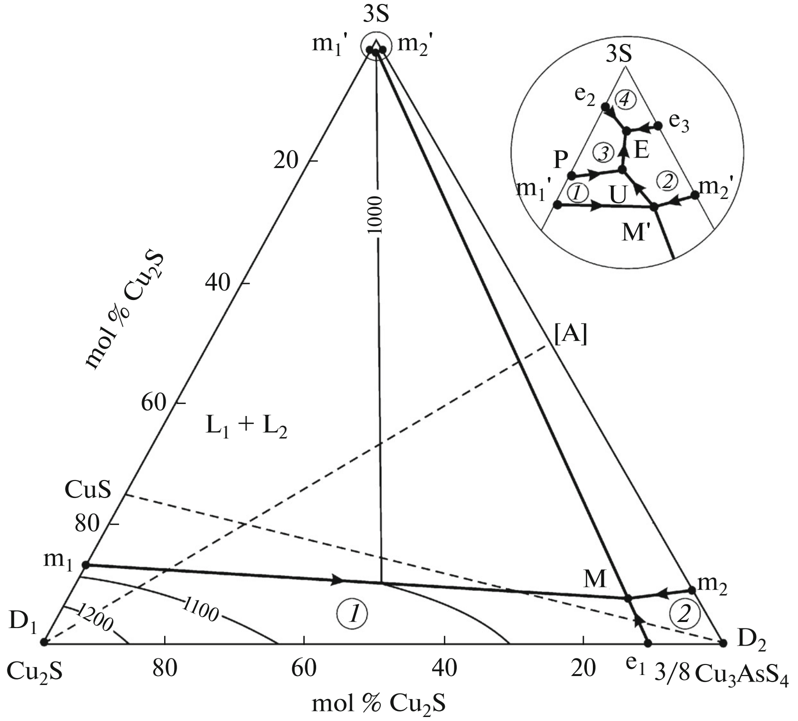

Fig. 3. Projection of the liquidus surface of the Cu_2S–Cu_3AsS_4–S system. Primary crystallization fields: (*1*) α", (*2*) Cu_3AsS_4, (*3*) CuS, and (*4*) S. The dashed lines are the studied polythermal sections.

equilibria α" ↔ α' + Cu_3AsS_4 and α' ↔ $(Cu_2S)_I$ + Cu_3AsS_4, respectively, are established.

Cu_3AsS_4–8S System (Fig. 1b) is characterized by the existence of monotectic ($m_2m'_2$) and eutectic (e_3) equilibria. At the monotectic temperature (960 K), the phase separation region extends from ~2 to 90 mol % Cu_3AsS_4. The eutectic is degenerate near the composition point of elemental selenium and crystallizes at 387 K.

Isothermal section at 300 K of the phase diagram of the Cu_2S–Cu_3AsS_4–S system is presented in Fig. 2. As is seen, the composition points of all the copper sulfides are connected by tie lines with the Cu_3AsS_4 point, which divide the concentration triangle into three-phase regions. The phase compositions of the alloys were confirmed by X-ray studies.

Liquidus surface (Fig. 3) of the Cu_2S–Cu_3AsS_4–S system comprises two fields characterizing the primary crystallization of the α"-phase and Cu_3AsS_4. The primary crystallization fields of CuS and elemental sulfur are degenerate. This part of the *T–x–y* diagram is shown in Fig. 3 in a magnified view (arbitrary scale).

A characteristic feature of this system is the wide region of phase separation ($L_1 + L_2$). It has the shape of a wide continuous zone between the monotectic horizontal lines of the lateral systems Cu_2S–S ($m_1m'_1$) and Cu_3AsS_4–S ($m_2m'_2$). The eutectic curve originating from the point e_1 intersects the phase separation region and transforms into the invariant monotectic equilibrium (horizontal line MM'). A number of invariant and monovariant equilibria are degenerate near the sulfur composition point. The table presents the types and temperatures of all the in- and monovariant equilibria in the system.

Polythermal Sections

We constructed some polythermal sections of the *T–x–y* diagram, which more clearly demonstrate crystallization processes and solid-phase transformations in the system. Let us consider them together with Figs. 1–3 and the table.

Section 4CuS–Cu_3AsS_4 (Fig. 4). The liquidus consists of two curves describing the primary crystallization of the α"-phase and Cu_3AsS_4. In the composition range 35–100 mol % CuS, the primary crystallization of the α"-phase occurs by the monovariant monotectic reaction m_1M. Below the liquidus, the crystallization continues initially by the monovariant monotectic reactions m_1M and e_1M and then by the invariant monotectic reaction M (950 K) and is completed by the invariant transition reaction U at 770 K (Fig. 3; table) to form the two-phase mixture CuS + Cu_3AsS_4.

Section Cu_2S–[A] (Fig. 5). As one of the initial components of this section, the two-phase alloy Cu_3AsS_4 + S of the composition [A] was chosen (Fig. 3).

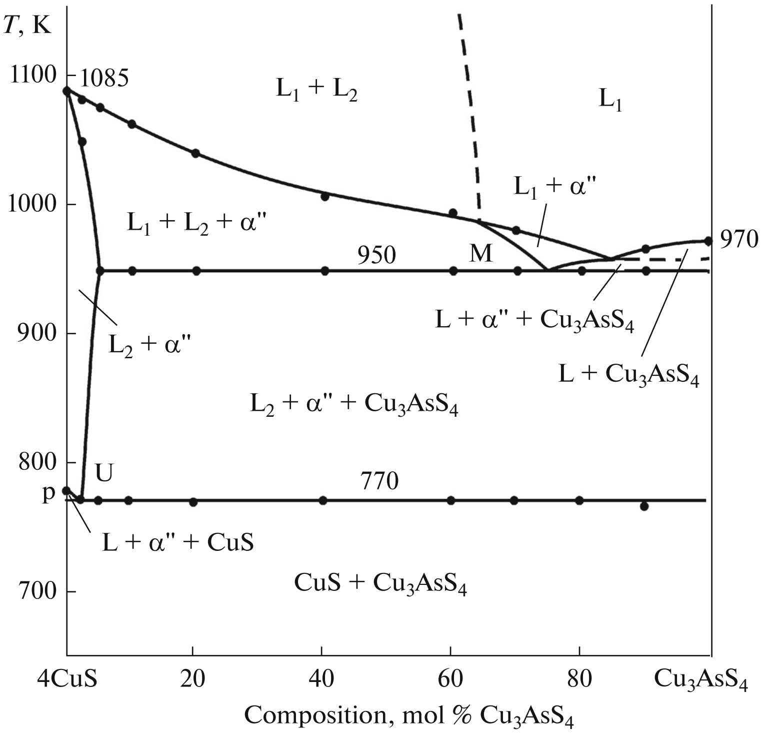

Fig. 4. Polythermal section $CuS–Cu_3AsS_4$ of the phase diagram of the $Cu_2S–Cu_3AsS_4–S$ system.

(a) Invariant and (b) monovariant equilibria in the $Cu_2S–Cu_3AsS_4–S$ system

a) Point in Fig. 3	Equilibrium	*T*, K
D_1	$L \leftrightarrow \alpha''$	1403
D_2	$L \leftrightarrow Cu_3AsS_4$	970
P_1	$L + \alpha'' \leftrightarrow CuS$	780
U_1	$L + \alpha'' \leftrightarrow CuS + Cu_3AsS_4$	770
e_1	$L \leftrightarrow \alpha'' + Cu_3AsS_4$	960
e_2	$L \leftrightarrow CuS + S$	388
e_3	$L \leftrightarrow Cu_3AsS_4 + S$	387
E	$L \leftrightarrow CuS + Cu_3AsS_4 + S$	385
$m_1(m'_1)$	$L_1 \leftrightarrow L_2 + \alpha''$	1086
$m_2(m'_2)$	$L_1 \leftrightarrow L_2 + Cu_3AsS_4$	960
M(M')	$L_1 \leftrightarrow L_2 + \alpha'' + Cu_3AsS_4$	950
b) Curve in Fig. 3	Equilibrium	*T*, K
e_1M; M'U	$L \leftrightarrow \alpha'' + Cu_3AsS_4$	960–950; 950–770
PU	$L + \alpha'' \leftrightarrow CuS$	780–770
UE	$L \leftrightarrow \alpha''(\alpha') + Cu_3AsS_4$	770–390
e_2E	$L \leftrightarrow CuS + S$	388–385
e_3E	$L \leftrightarrow Cu_3AsS_4 + S$	387–385
$m_1M(m'_1M')$	$L_1 \leftrightarrow L_2 + \alpha''$	1086–960
$m_2M(m'_2M')$	$L_1 \leftrightarrow L_2 + Cu_3AsS_4$	960–950

α' and α" are solid solutions based on the intermediate and high-temperature modifications of Cu_2S, respectively.

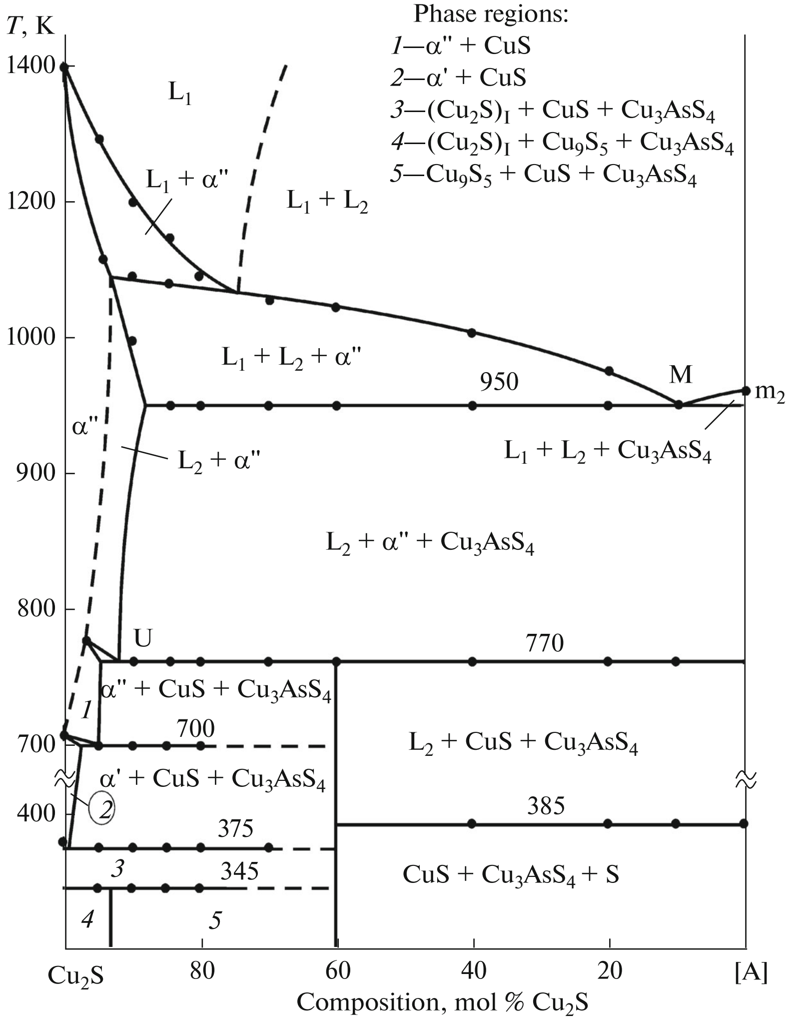

Fig. 5. Polythermal section Cu$_2$S–[A] of the phase diagram of the Cu$_2$S–Cu$_3$AsS$_4$–S system.

This section intersects almost all the phase regions (Fig. 2) and represents most of the in- and monovariant equilibria in the studied system. Over wide composition ranges from the melt L$_1$ (~75–100 mol % Cu$_2$S) or two separating liquid phases L$_1$ + L$_2$ (~10–75 mol % Cu$_2$S), the α''-phase primarily crystallizes. Within the composition range 0–10 mol % Cu$_2$S by the monotectic reaction m$_2$M, the compound Cu$_3$AsS$_4$ primarily crystallizes. The crystallization continues invariantly by the monotectic (M) and transition (U) reactions. Within the composition range ~60–95 mol % Cu$_2$S, the crystallization is completed with the reaction U to produce the three-phase region α'' + CuS + Cu$_3$AsS$_4$. At concentrations <60 mol % Cu$_2$S, the crystallization is completed with the eutectic reaction E (385 K) to form the three-phase mixture CuS + Cu$_3$AsS$_4$ + S.

The thermal events at 700 and 375 K correspond to the eutectoid equilibria α'' ↔ α' + Cu$_3$AsS$_4$ and α' ↔ (Cu$_2$S)$_I$ + Cu$_3$AsS$_4$, respectively, and the thermal event at 350 K characterizes the solid-phase reaction (Cu$_2$S)$_I$ + CuS = Cu$_9$S$_5$. This reaction gives rise to the three-phase regions (Cu$_2$S)$_I$ + Cu$_9$S$_5$ + Cu$_3$AsS$_4$ and Cu$_9$S$_5$ + CuS + Cu$_3$AsS$_4$ (Fig. 2).

Thus, the Cu$_2$S–Cu$_3$AsS$_4$–S subsystem is a subordinate triangle in the ternary system Cu–As–S. The liquidus surface consists of the primary crystallization fields of the high-temperature modification of Cu$_2$S, Cu$_3$AsS$_4$, CuS, and S. The last two surfaces are degenerate near the composition point of elemental sulfur. In the system, there is a wide region of phase separation, which covers over 90% of the liquidus surface area. At room temperature, in the system, there exist three three-phase regions divided by the tie lines Cu$_9$S$_5$ + Cu$_3$AsS$_4$ and CuS + Cu$_3$AsS$_4$.

ACKNOWLEDGMENTS

This work was supported by the Science Foundation of the State Oil Company of Azerbaijan Republic (project "Production and Investigation of New Functional Materials Based on Multicomponent Metal Chalcogenides for Alternative Energy Sources and Electronics," 2014).

REFERENCES

1. M. A. Popesku, *Non-Crystalline Chalcogenides* (Springer Netherlands, Dordrecht, Netherlands, 2000).
2. M. B. Babanly, Yu. A. Yusibov, and V. T. Abishev, *Ternary Chalcogenides Based on Copper and Silver* (Bakinsk. Gos. Univ., Baku, 1993) [in Russian].
3. M. Rikel, M. Harmelin, and A. Prince, *Arsenic–Copper–Sulfur*, in *Ternary Alloys*, Ed. by G. Petzow, G. Effenberg, and F. Aldinger (VCH, Weinheim, 1994), Vol. 10, pp. 109–127.
4. N. I. Kopylov and Yu. D. Kaminskii, *Arsenic* (Sib. Univ. Izd-vo, Novosibirsk, 2004) [in Russian].
5. D. Filippou, P. Germain, and T. Grammatikopoulos, Miner. Proc. Extract. Met. Rev. **28**, 247 (2007).
6. S. Maske and B. J. Skinner, Econ. Geol. **66**, 901 (1971).
7. B. Gather and R. Blachnic, J. Less-Common Met. **48**, 205 (1976).
8. N. I. Kopylov, S. M. Minkevich, M. Z. Toguzov, and D. V. Smailov, Zh. Neorg. Khim. **20**, 3393 (1975).
9. G. Kurz and R. Blachnik, J. Less-Common Met. **155**, 1 (1989).
10. A. Müller and R. Blachnik, Thermochim. Acta **387**, 153 (2002).
11. A. Müller and R. Blachnik, Z. Anorg. Allg. Chem. **629**, 1833 (2003).
12. Z. T. Gasanova, Z. S. Aliev, Yu. A. Yusibov, and M. B. Babanly, Russ. J. Inorg. Chem. **57**, 1158 (2012).
13. M. B. Babanly, Z. T. Gasanova, L. F. Mashadieva, et al., Inorg. Mater. **48**, 225 (2012).
14. *Binary Alloy Phase Diagrams*, Ed. by T. B. Massalski and H. Okamoto (ASM International, Materials Park, Ohio, 1990).
15. *State Diagrams of Binary Metal Systems: Handbook*, Ed. by N. P. Lyakishev (Mashinostroenie, Moscow, 1997), Vol. 2 [in Russian].
16. Yu. V. Voroshilov, T. L. Evstigneeva, and I. Ya. Nekrasov, *Crystal Chemical Tables of Ternary Chalcogenides* (Nauka, Moscow, 1989) [in Russian].
17. J. Emsley, *The Elements* (Oxford Univ. Press, Oxford, 1991).
18. V. M. Glazov, A. S. Burkhanov, and N. M. Saleeva, Izv. Akad. Nauk SSSR, Neorg. Mater. **13**, 917 (1977).

Translated by V. Glyanchenko